https://cimav.repositorioinstitucional

Textured Multiferroics: 2-D Diffraction and Properties Prediction

A. Muñoz-Romero, L. Fuentes-Montero, M.E. Montero-Cabrera, U. Trivedi, L.E. Fuentes-Cobas

Abstract

A description of recent work performed by collaboration among the CIMAV Crystal Physics Group, the ANSTO Bragg Institute, the ILL Diffraction Group and the GEC Nanotechnology Education and Research Centre (NERC), regarding structure-electromagnetic properties relationships, is given. Structure analysis puts emphasis on thin films texture characterization. The new software package *ANAELU*, for texture analysis via two-dimensional (2-D) diffraction detection, is described. Crystallographic texture plays a significant role on ferroic and multiferroic bulk and nano-structured materials properties. With the objective of estimating effective values for polycrystal dielectric, piezoelectric, elastic and magnetoelectric coefficients, the Voigt, Reuss and Hill approximations are systematized in an extended version of program *SAMZ*.

Indtroduction

The aim of the present paper is to divulge recent developments performed by our collaborative group in the field of texture measurement and on the characterization of the texture effect on electromagnetic properties.

The first part of the article presents the manner used by the group to describe by means of surface representations: a) physical properties of anisotropic (singleor

polycrystal) materials and b) textured polycrystals' inverse pole figures (IPF). The second and final section exposes the computer simulation of a hypothetical case in which a given fibre texture leads to a modelled 2-D diffraction pattern and to the calculation of the effective dielectric constant under various approximations.

Surface representation of properties and IPFs

So-called longitudinal surface representation of physical properties is performed by means of symmetrized spherical harmonics expansions. Mathematical tools provided by Bunge [1] are implemented in the Matlab code *SAMZ* (singleand polycrystal modules [2]). Symmetry implications follow the selection rules given by the International Tables for Crystallography [3], with particular consideration of the polar/axial nature of properties and the magnitudes' behaviour under space/time inversion [4].

Properties are classified according to the rank and the nature of their associated tensors. Electro-elasto-thermo-magnetic properties represented by *SAMZ* are: specific heat, permittivity, permeability, elasticity, thermal expansion, pyroelectricity, pyromagnetism, piezoelectricity, piezomagnetism and magnetoelectricity. The matrix representations of all the mentioned properties, for the 32 ordinary symmetry and the 90 magnetic symmetry point groups, are considered.

Fig. 1 shows, as an example, the surface representation of the longitudinal magnetoelectric coefficient of a $LiCoPO_4$. The magnetic point group is $D_{2h}(C_{2v})$ = 2'/m 2'/m 2/m'.

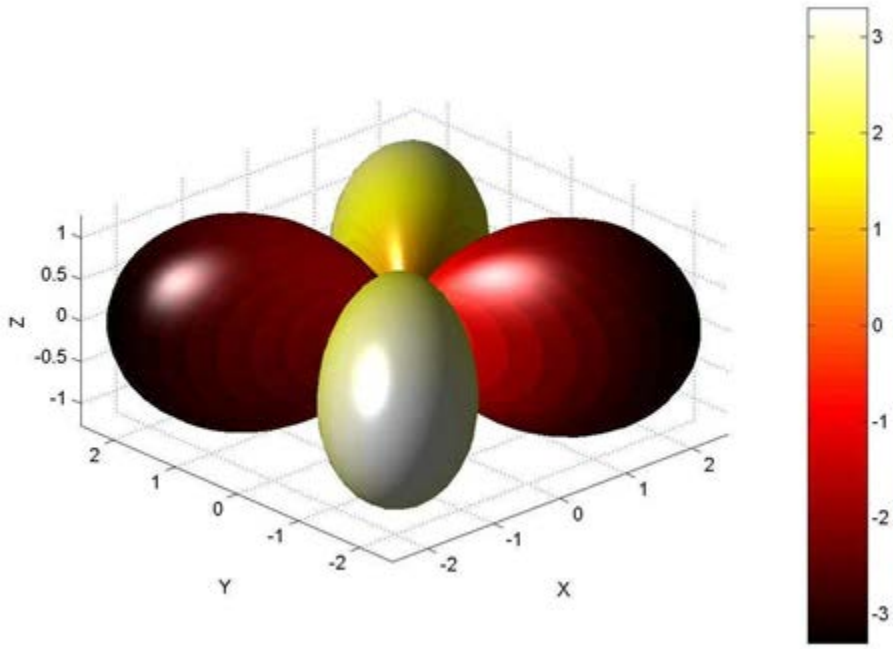

Fig. 1: $LiCoPO_4$ longitudinal magnetoelectric coefficient. Tensor components are $\alpha_{12} = 18$; $\alpha_{21} = 31$ (ps/m) [5].

Due to the axial and time reversible nature of magnetoelectricity, the vertical mirror planes x = 0 and y = 0 transform positive lobes into negative ones.

Fibre textures, frequently found in axially-pressed electroceramics, are represented by their IPFs. IPFs are modelled as Gaussian or March-Dollase bell-shaped surfaces [6], with given widths and fulfilling: a) Laue symmetry (as in normal diffraction) and b) normalization conditions. Fig. 2 shows an example of IPF modelling.

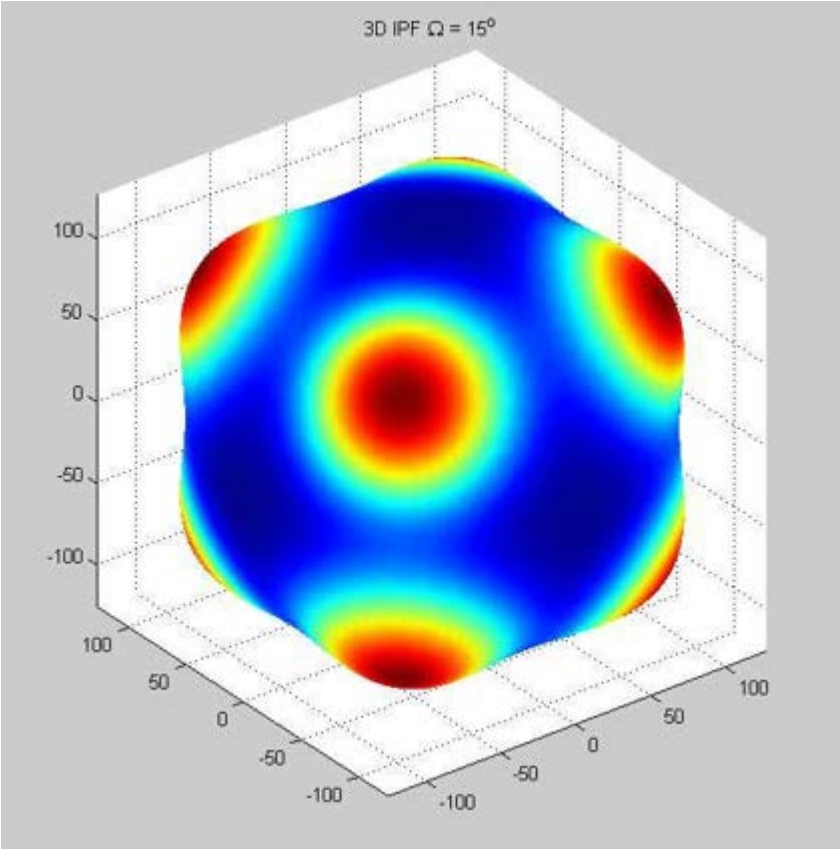

Fig. 2: $BaTiO_3$ fibre texture IPF. Gaussian (1, 1, 1) preferred orientation, distribution width = 15°. Multiplicity of the (1, 1, 1) pole for C_{4v} = 4mm symmetry is generated by *SAMZ*.

Modelling a particular case: $BaTiO_3$ polycrystal dielectric constant

The following section illustrates the treatment given to textured polycrystals effective properties.

Fig. 3 shows in surface representation the longitudinal dielectric constant of a $BaTiO_3$ single crystal.

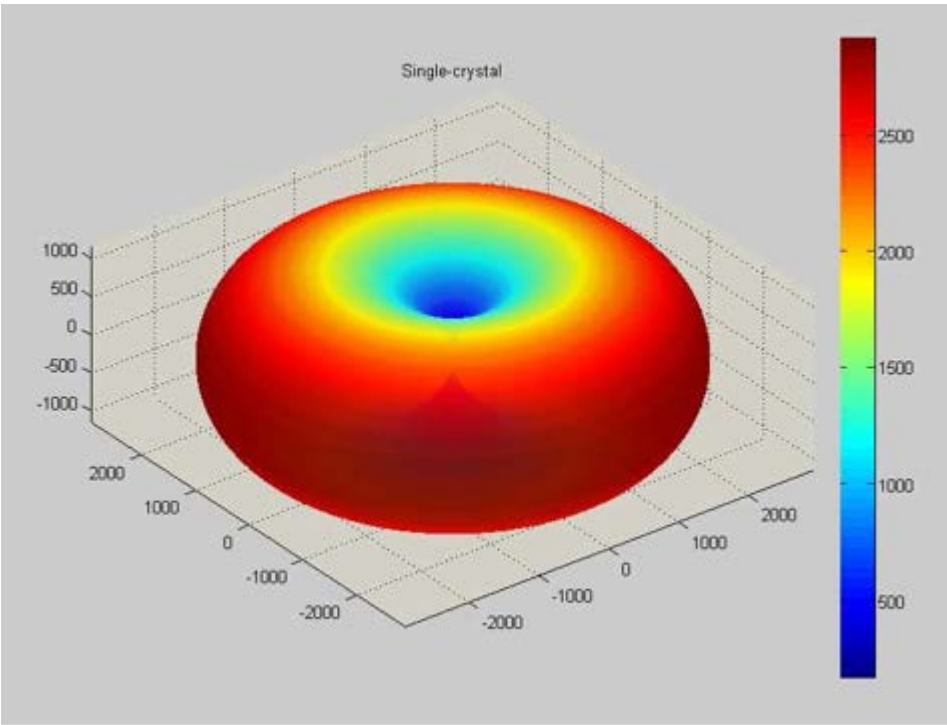

Fig. 3: BaTiO3 single-crystal dielectric constant surface. Tensor components are $K_{11} = K_{22} = 2{,}920$; $K_{33} = 168$ [7].

The anisotropy of the considered material's property is remarkable.

Inverse tensors, in this case the impermittivity $\boldsymbol{\beta} = \mathbf{K}^{-1}$, is required for effective properties calculations. $BaTiO_3$ impermittivity surface is shown in Fig. 4.

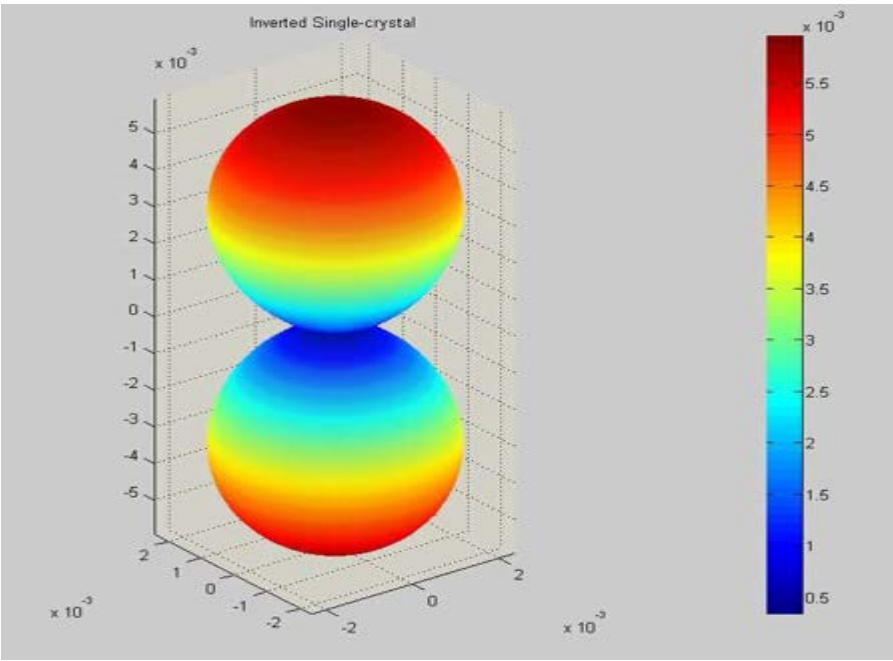

Fig. 4: Longitudinal surface representation of $BaTiO_3$ single-crystal impermittivity $\boldsymbol{\beta} = \mathbf{K}^{-1}$.
The tensor components are $\beta_{11} = \beta_{22} = 3.42 \cdot 10^{-4}$; $\beta_{33} = 0.006$

Texture measurement in ferroic thin films may be performed by means of grazing-incidence diffraction experiments. Two-dimensional (2-D) detection of diffracted synchrotron radiation is particularly useful in this field. Software package *ANAELU* [8], recently produced by our group, is a modelling tool that allows the analysis and the interpretation by modelling of 2-D diffraction patterns produced by textured samples. Fig. 5 shows the calculated 2-D pattern of a hypothetical $BaTiO_3$ thin film with (0, 0, 1) fibre texture.

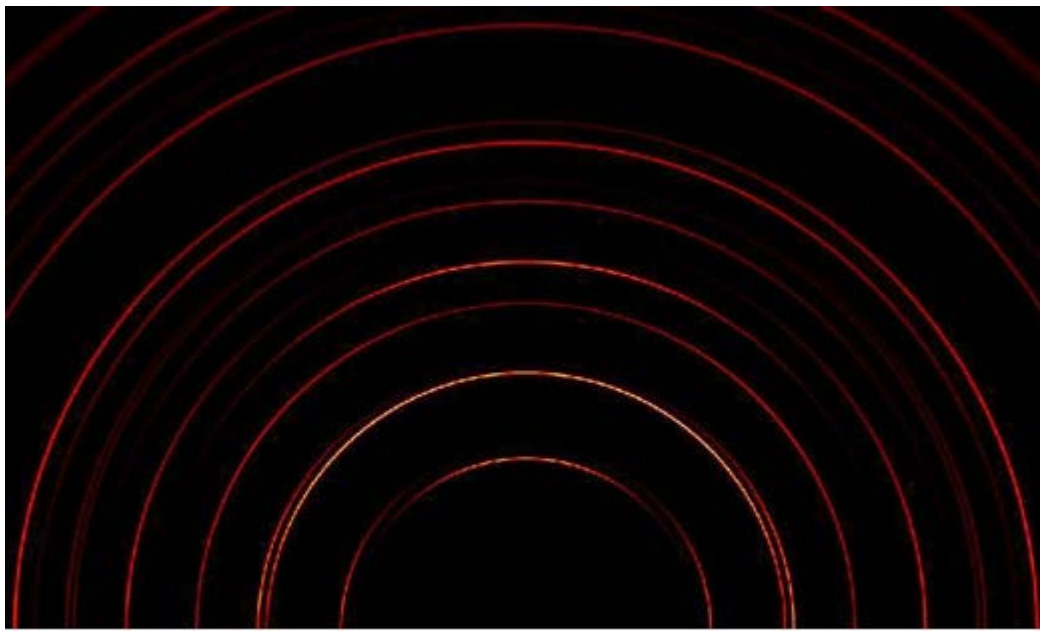

Fig. 5: Output from program *ANAELU* for 2-D diffraction analysis. Model sample: $BaTiO_3$, textured thin film. Fibre texture characteristics: Preferred crystal direction: $\mathbf{h}_0 = 0, 0, 1$.
Angular width of the Gaussian orientation distribution: $\Omega = 30°$.
Hypothetical experiment: $\lambda = 1$ Å, sample-detector distance = 125 mm.
The non-uniform distribution of intensities along the Debye rings is readily seen.

Polycrystal physical properties are single-crystal ones, modulated by texture, stereography and other factors. Regarding fibre textures, knowledge of the symmetry axis IPF allows several averaging procedures to predict the so-called

effective polycrystal properties. Following Bunge's symmetrized spherical harmonics treatment, the longitudinal surface representation of average properties may be calculated according to the Voigt ("parallel" configuration), Reuss ("series" configuration) and Hill (Voigt and Reuss average) approximations [9].

Fig. 6 displays the mean dielectric constant of the hypothetical $BaTiO_3$ fibre texture of Fig. 5, calculated by the polycrystal module of *SAMZ*, according to the Voigt average. In the considered case, the electric field intensity **E** is considered invariant in the sample volume.

Fig. 7 shows the dielectric constant dependence on the polar angle for the considered sample in the Voigt, Reuss (constant electric displacement **D**) and Hill approximations.

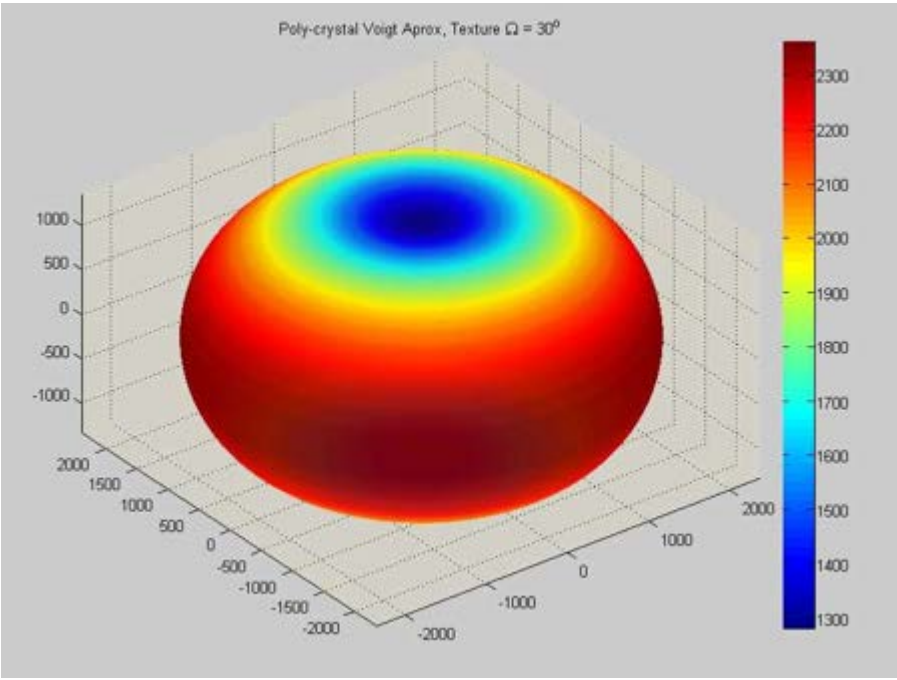

Fig. 6: Mean longitudinal dielectric constant for a BaTiO3 polycrystal. Gaussian (0, 0, 1) fibre texture with characteristic width Ω = 30°. Voigt average (parallel configuration, constant electric field intensity assumed).

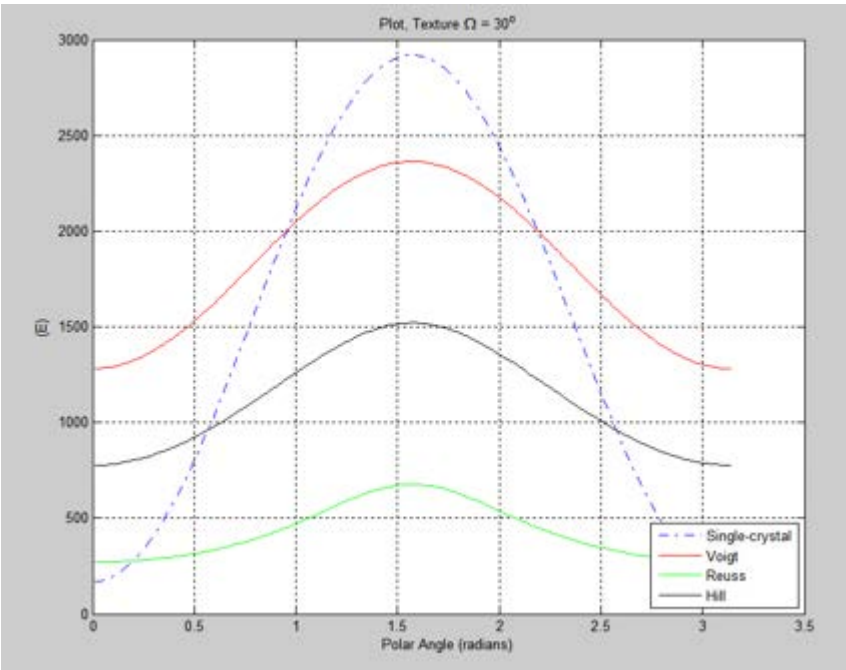

Dielectric constant dependence on polar angle.
Voigt, Reuss and Hill approximations for the hypothetical sample of Figs. 5 and 6.

Conclusions

A methodology for the predictive estimation of diffraction-based effective properties of fibretextured materials has been briefly discussed. Associated computer programs (*SAMZ* and *ANAELU*) were described and a case study was exposed. Presented software packages are freely downloadable from the CIMAV software web page [10].

Acknowledgements

Present investigation has been supported by the Mexican Consejo Nacional de Ciencia y Tecnología (CONACYT), Project 102171 “Nano-multiferroics”.

References

[1]H.J. Bunge, Texture Analysis in Materials Science, Butterworths, London, 1982.

[2]L. Fuentes, A. Rodríguez, et al., Integr. Ferroelec. 71 (2005) 289 – 301.

[3]A. S. Borovik-Romanov, H. Grimmer, A. Authier (ed.), International Tables Crystallogr., Vol. D, Physical Properties of Crystals, Section 1.5, Magnetic Properties, Kluwer, Dordrecht, 2003.

[4]L. Fuentes-Cobas, J. Matutes-Aquino, M.E. Fuentes Montero, K.H.J. Buschow (ed.), Handbook Magnetic Materials, Vol. 19, Chap 3, Magnetoelectricity, 129-229, Elsevier, Amsterdam (2011).

[5] T.B.S. Jensen, N.B. Christensen et al., Phys. Rev. B 79 (2009) 92412.

[6]L.Fuentes-Cobas, L. Pardo (ed.), Multifunctional Polycrystalline Ferroelectric Materials, Chap. 6, Synchrotron Radiation Diffraction and Scattering in Ferroelectrics, Springer, London (2011).

[7] W. D. Kingery, et al., Introduction to Ceramics, 2nd ed., John Wiley & Sons, New York, 1976.

[8] L. Fuentes-Montero, M. E. Montero-Cabrera, L. Fuentes-Cobas. J. Appl. Cryst. 44 (2011) 241.

[9] H.J. Bunge, R. Kiewel, Th. Reinert et al, J. Mechanics and Physics of Solids. 48 (2000) 29.

[10] http://www.cimav.edu.mx/investigacion/software